arXiv:quant-ph/0504147v1 20 Apr 2005

Phase-dependent interference mechanisms in a three-level Λ system driven by a quantized laser field

Jörg Evers*
Max-Planck-Institut für Kerphysik, Saupfercheckweg 1, D-69117 Heidelberg, Germany

The dynamics of an atomic few-level system can depend on the phase of driving fields coupled to the atom if certain conditions are satisfied. This is of particular interest to control interference effects, which can alter the system properties considerably. In this article, we discuss the mechanisms of such phase control and interference effects in an atomic three-level system in Λ configuration, where the upper state spontaneously decays into the two lower states. The lower states are coupled by a driving field, which we treat as quantized. This allows for an interpretation on the single photon level for both the vacuum and the driving field. By analyzing the system behavior for a driving field initially in non-classical states with only few Fock number states populated, we find that even though the driving field is coupled to the lower states only, it induces a multiplet of upper states. Then interference occurs independently in three-level subsystems in V configuration, each formed by two adjacent upper states and a single dressed lower state.

PACS numbers: 42.50.Lc,42.50.Ct,42.50.Hz

I. INTRODUCTION

Interference is recognized as a major mechanism to control quantum dynamics [1]. If a system exhibiting quantum interference is sensitive to the phase of applied driving fields, then the interference itself can often be conveniently controlled. This is intuitively clear, as the relative phase between the interfering pathways decides whether constructive or destructive interference takes place. Thus it is not surprising that phase-dependent systems have been discussed extensively [1, 2, 3, 4, 5, 6, 7, 8, 9, 10, 11, 12, 13, 14, 15, 16, 17, 18]. The phase-control of quantum interference has also been verified experimentally [18]. One of the first and simplest examples for a phase-sensitive system is a three-level system in Λ configuration, where the upper state decays spontaneously into the two lower states coupled by a classical driving field [2]. The transition dipole moments from the upper state to the two lower states are assumed to be non-orthogonal. Then, due to the driving field, each of the two lower states can be reached via two pathways: Either by a direct spontaneous decay, or by a decay into the other state followed by a driving field-induced transition. The two paths interfere, with a relative phase between the two path amplitudes equal to the driving field phase. This classical interpretation, however, is unsatisfactory for several reasons. First, the respective initial and the final states of two interfering pathways are obviously not the same, as one involves an interaction with the driving field, whereas the other does not. Thus one could argue that the two paths do not interfere, as they could be distinguished by a measurement. A typical counter-argument against this is that the photon number distribution of a strong coherent driving field has a large width, such that the two paths cannot be distinguished. This argument, however, cannot be verified using a semi-classical description of the system. Second, while it is clear that the two pathways must have either a different initial or a different final state, it is not apparent in the semiclassical description what the exact pathways are. Third, the classical description restricts the system to classical driving fields, and thus does not allow to consider non-classical driving fields to further study the system properties. Finally, it is not obvious where the phase of the driving field should be considered in a quantized treatment. For example, in the quantized treatment, both the coupling constants and the initial field state can carry phase information.

Thus in this article, we revisit the three-level system

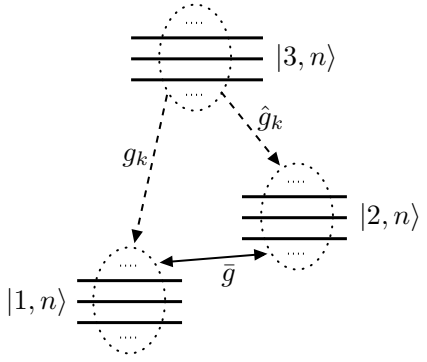

FIG. 1: Bare-state representation of the considered system. The multiple lines for each state denote the Fock state multiplets induced by the coupling of the atom with a quantized driving field. The upper states $|3,n\rangle$ decay spontaneously into the two lower state multiplets $|1,n\rangle$ and $|2,n\rangle$. Here, n is the number of photons in the respective driving field Fock modes. The two lower state multiplets are coupled by the quantized driving field. g_k and $\hat{g}_k$ are coupling constants for the interaction with the vacuum giving rise to spontaneous emission, $\bar{g}$ is the coupling constant for the driving field.

*Electronic address: joerg.evers@mpi-hd.mpg.de

in Λ configuration, but treat the driving field as quantized. This allows to discuss the phase and interference effects on the single photon level. We derive a set of equations for the two dressed lower states alone, and solve this numerically for different field configurations. For coherent fields, which are closest to classical fields, we find the same results as in the classical case. By analyzing driving fields consisting of a single Fock mode, few adjacent number states, or separated Fock states, it is possible to find the origin of the quantum interference and to identify the interfering pathways. It turns out that it is not the large total width of the photon number distribution which is crucial for the interference, but rather a fixed phase relation (coherence) between adjacent Fock modes. The driving field gives rise to an upper state multiplet, even though it is only coupled to the lower state [19, 20, 21]. Then the interference occurs independently in three-level subsystems in V-configuration, which are formed by two adjacent upper states and a single lower dressed state. Finally, some insight is gained in the role of phase in quantum systems by comparing the quantum treatment with the semiclassical description.

The article is organized as follows: In the next section II, we analytically derive a set of equations for the two dressed ground states alone, which is then solved numerically in Section III for different initial field configurations. The results of this analysis are discussed and summarized in Section IV.

II. ANALYTICAL CONSIDERATIONS

In the following, we consider a three-level system in Λ-configuration as shown in Fig. 1. The upper state $|3\rangle$ decays to the two lower states $|1\rangle$, $|2\rangle$ with decay rates γ_1, γ_2, respectively. In addition, the two lower states are connected by a coherent field, which in the following we treat as a quantized field. For simplicity, we assume the driving field to be on resonance with the transition frequency ω_{21} between the two lower states. The interaction Hamiltonian in the interaction picture may then be written as [22]

$$V(t) = V_{\rm drive} + V_{\rm SE}(t)\,, \tag{1}$$

where

$$V_{\rm drive} = i\hbar\left(\bar{g}A_{21}b - \bar{g}^* A_{12}b^\dagger\right)\,, \tag{2}$$

$$V_{\rm SE}(t) = i\hbar\sum_k \Big(g_k A_{31}a_k e^{-i\delta_k t} - g_k^* A_{13}a_k^\dagger e^{i\delta_k t} + \hat{g}_k A_{32}a_k e^{-i\hat{\delta}_k t} - \hat{g}_k^* A_{23}a_k^\dagger e^{i\hat{\delta}_k t}\Big)\,. \tag{3}$$

Here, $V_{\rm SE}(t)$ denotes the interaction of the atom with the surrounding vacuum field giving rise to spontaneous emission, and $V_{\rm drive}$ describes the interaction with the quantized driving field. $A_{ij} = |i\rangle\langle j|$ $(i,j \in \{1,2,3\})$ are atomic transition operators, b $(b^\dagger)$ are annihilation (creation) operators of the driving field, and a_k $(a_k^\dagger)$ are the corresponding operators of the surrounding vacuum mode k. $\delta_k = \omega_k - \omega_{31}$ and $\hat{\delta}_k = \omega_k - \omega_{32}$ are detunings to atomic transition frequencies $\omega_{ij} = \omega_i - \omega_j$, where $\hbar\omega_i$ is the energy of state $|i\rangle$. $\bar{g}, g_k$ and $\hat{g}_k$ are coupling constants. As we are interested in the phase-dependence of the system, these constants are treated as complex entities. In particular, we define

$$\bar{g} = |\bar{g}|\, e^{i\phi}\,. \tag{4}$$

Note that for simplicity, we treat the transitions between the two lower atomic states as one-photon transitions [2]. However, replacing $V_{\rm drive}$ with a corresponding effective Hamiltonian containing two-photon transitions proportional to bb $(b^\dagger b^\dagger)$ does not change the involved physics. The interference effects in this system crucially depend on the relative orientation of the dipole moments of the transitions $|3\rangle \leftrightarrow |1\rangle$ and $|3\rangle \leftrightarrow |2\rangle$. If the two dipole moments are orthogonal, then no interference effects are possible. A simple interpretation for this result is that then the photons emitted spontaneously on the two transitions can be distinguished by their polarizations, such that no pathway interference is possible. Thus in the following, we assume the two dipole moments to be parallel. Note that spontaneously generated coherences between the two lower states which arise if further ω_{21} is smaller than or of the same order as γ_1, γ_2 do not play a role in the current system setup. These coherences, however, become relevant if additional driving fields on transitions $|3\rangle \leftrightarrow |i\rangle$ $(i \in \{1,2\})$ couple to them (see, e.g., [23]).

To simplify the analysis, we transfer the system to the dressed state representation for the two driven states, which is given by

$$|+,n\rangle = \frac{1}{\sqrt{2}}\left(|1,n+1\rangle + i\,e^{i\phi}\,|2,n\rangle\right)\,, \tag{5a}$$

$$|-,n\rangle = \frac{1}{\sqrt{2}}\left(|1,n+1\rangle - i\,e^{i\phi}\,|2,n\rangle\right)\,. \tag{5b}$$

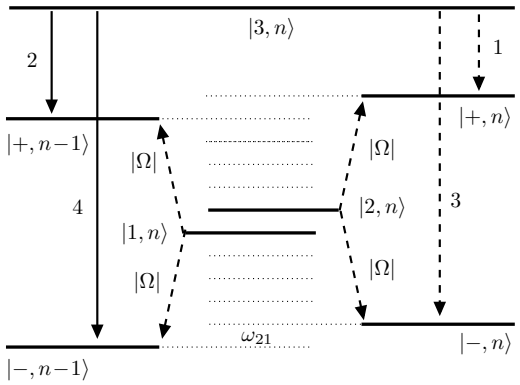

FIG. 2: Dressed state representation of the system configuration with a quantized driving field. The two lower bare states $|1\rangle$, $|2\rangle$ are AC-Stark shifted and absorbed into the dressed states due to the driving field. The numbers at the arrows correspond to the numbers at the peaks in Fig. 4.

The dressed-state representation of the system is shown in Fig. 2 for parameters where the AC-Stark splitting is larger than the level splitting of the two lower bare states.

The wave function of the system can be written as

$$|\Psi(t)\rangle = \sum_n C_3^n(t)\,|3,n,0\rangle + \sum_{n,k} \alpha_k^n(t)\,a_k^\dagger\,|+,n,0\rangle + \sum_{n,k} \beta_k^n(t)\,a_k^\dagger\,|-,n,0\rangle\,. \tag{6}$$

Here, $|i,n,0\rangle$ denotes a state with no photons in the surrounding vacuum, n photons in the driving field mode and the atom in electronic state i ($i = 3,+,-$). From the Schrödinger equation,

$$i\hbar\frac{d}{dt}\,|\Psi(t)\rangle = V(t)\,|\Psi(t)\rangle\,, \tag{7}$$

the equations of motion for the state amplitudes can be evaluated to give

$$\frac{d}{dt}\,C_3^n(t) = \frac{1}{\sqrt{2}}\sum_k g_k\,e^{-i\delta_k t}\,\left(\alpha_k^n(t)+\beta_k^n(t)\right) + \frac{i}{\sqrt{2}}\sum_k \hat{g}_k\,e^{i\phi}\,e^{-i\hat{\delta}_k t}\,\left(\alpha_k^n(t)-\beta_k^n(t)\right)\,, \tag{8}$$

$$\frac{d}{dt}\,\alpha_k^n(t) = -\frac{1}{\sqrt{2}}\,C_3^n(t)\left(g_k^*\,e^{i\delta_k t} + i\hat{g}_k^*\,e^{-i\phi}\,e^{i\hat{\delta}_k t}\right) - \frac{i}{2}\,|\bar{g}|\,\sqrt{n+1}\left(\alpha_k^{n+1}(t)+\beta_k^{n+1}(t)\right) - \frac{i}{2}\,|\bar{g}|\,\sqrt{n}\,\left(\alpha_k^{n-1}(t)-\beta_k^{n-1}(t)\right)\,, \tag{9}$$

$$\frac{d}{dt}\,\beta_k^n(t) = -\frac{1}{\sqrt{2}}\,C_3^n(t)\left(g_k^*\,e^{i\delta_k t} - i\hat{g}_k^*\,e^{-i\phi}\,e^{i\hat{\delta}_k t}\right) + \frac{i}{2}\,|\bar{g}|\,\sqrt{n+1}\left(\alpha_k^{n+1}(t)+\beta_k^{n+1}(t)\right) - \frac{i}{2}\,|\bar{g}|\,\sqrt{n}\,\left(\alpha_k^{n-1}(t)-\beta_k^{n-1}(t)\right)\,. \tag{10}$$

As shown in Appendix A, in a Wigner-Weisskopf-like evaluation, and assuming that the atom initially is in the upper state $|3\rangle$ ($\alpha_k^n(0) = 0 = \beta_k^n(0)$), one may solve the equation of motion for the upper state amplitudes to give

$$C_3^n(t) = C_3^n(0)\,e^{-\frac{1}{2}\gamma t}\,. \tag{11}$$

The rate $\gamma = \gamma_1 + \gamma_2$ is the total decay rate of the upper state $|3\rangle$ to both lower states. Note that each of the Fock number state amplitudes of the driving field decays independently. The reason is that the spontaneous emission from the upper state is an irreversible process, such that the driving field coupling to the lower states cannot influence the decay of the upper states. As the Wigner-Weisskopf procedure involves the continuum limit of an infinite quantization volume, in the following, we replace the discrete ground state amplitudes and the detunings by their continuous counterparts:

$$\alpha_k^n(t) \longrightarrow \alpha_\omega^n(t)\,, \qquad \beta_k^n(t) \longrightarrow \beta_\omega^n(t)\,, \tag{12}$$

$$\delta_k \longrightarrow \delta_\omega = \omega - \omega_{31}\,, \tag{13}$$

$$\hat{\delta}_k \longrightarrow \hat{\delta}_\omega = \omega - \omega_{32}\,. \tag{14}$$

On inserting Eq. (11) in Eqs. (9), (10), for each spontaneous emission frequency k, one obtains a set of coupled equations for the ground state coefficients $\alpha_k^n(t)$ and $\beta_k^n(t)$ alone, which can be solved numerically for any given initial state:

$$\frac{d}{dt}\,\alpha_\omega^n(t) = -\frac{1}{\sqrt{2}}\,C_3^n(0)\,e^{-\frac{1}{2}\gamma t}\,\Big\{g(\omega_{31})^*\,e^{i\delta_\omega t} + i\hat{g}(\omega_{32})^*\,e^{-i\phi}\,e^{i\hat{\delta}_\omega t}\Big\} - \frac{i}{2}\,|\bar{g}|\,\sqrt{n+1}\left(\alpha_\omega^{n+1}(t)+\beta_\omega^{n+1}(t)\right) - \frac{i}{2}\,|\bar{g}|\,\sqrt{n}\,\left(\alpha_\omega^{n-1}(t)-\beta_\omega^{n-1}(t)\right)\,, \tag{15}$$

$$\frac{d}{dt}\,\beta_\omega^n(t) = -\frac{1}{\sqrt{2}}\,C_3^n(0)\,e^{-\frac{1}{2}\gamma t}\,\Big\{g(\omega_{31})^*\,e^{i\delta_\omega t} - i\hat{g}(\omega_{32})^*\,e^{-i\phi}\,e^{i\hat{\delta}_\omega t}\Big\} + \frac{i}{2}\,|\bar{g}|\,\sqrt{n+1}\left(\alpha_\omega^{n+1}(t)+\beta_\omega^{n+1}(t)\right) - \frac{i}{2}\,|\bar{g}|\,\sqrt{n}\,\left(\alpha_\omega^{n-1}(t)-\beta_\omega^{n-1}(t)\right)\,. \tag{16}$$

Note that for typical atomic setups, one has $g(\omega_{31}) \approx \hat{g}(\omega_{32})$, which we assume in the following. From the ground state amplitudes, the spontaneous emission spectrum $S(\omega)$ may then be evaluated as

$$S(\omega) \propto \sum_n \left(|\alpha_\omega^n(t\to\infty)|^2 + |\beta_\omega^n(t\to\infty)|^2\right)\,, \tag{17}$$

where $\alpha_\omega^n(t\to\infty)$ and $\beta_\omega^n(t\to\infty)$ are the steady states of the ground state amplitudes. It is interesting to note that the expression for the emission spectrum Eq. (17) includes contributions both from the independent decay of the two transitions from the upper state and of interference terms, though somewhat hidden. On expanding Eq. (17), one obtains terms proportional to $|g(\omega_{31})|^2$ and to $|\hat{g}(\omega_{32})|^2$, which correspond to the independent spontaneous decay rates γ_1 and γ_2, respectively. Additionally, the spectrum contains contributions proportional to $g(\omega_{31})\hat{g}(\omega_{32})^*$ and $g(\omega_{31})^*\hat{g}(\omega_{32})$, which are the interference terms. If the two transition dipole moments $|3\rangle \leftrightarrow |i\rangle$ ($i \in \{1,2\}$) are assumed to be orthogonal, then these interference contributions vanish.

III. NUMERICAL ANALYSIS

In this section, we numerically solve the set of equations Eqs. (15),(16) for several cases of the initial distribution of Fock number states of the driving field. In particular, we compare the results to those obtained from a

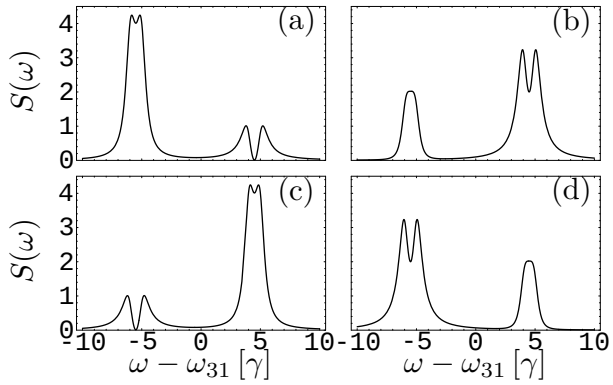

FIG. 3: Reference figures obtained using a classical driving field. $S(\omega)$ is the spontaneous emission spectrum of the system shown in Fig. 1. The parameters are $|\Omega| = 5\,\gamma, \omega_{21} = \gamma$, and the driving field phase ϕ_c is (a) $\phi_c = 0$, (b) $\phi_c = 0.5\,\pi$ and (c) $\phi_c = \pi$ and (d) $\phi_c = 1.5\,\pi$.

calculation involving a classical driving field, where $V_{\rm drive}$ is replaced by the classical interaction picture Hamiltonian [2]

$$V_{\rm drive}^{\rm class.} = i\hbar\,(\Omega\,A_{21} - \Omega^*\,A_{12})\ . \qquad (18)$$

Here, $\Omega = |\Omega|\,e^{i\phi_c}$ is the Rabi frequency for a classical field with phase ϕ_c. Using the classical Hamiltonian Eq. (18), for $|\Omega| = 5\,\gamma$ and $\omega_{21} = \gamma$, we obtain four reference figures shown in Fig. 3 for (a) $\phi_c = 0$, (b) $\phi_c = 0.5\,\pi$ and (c) $\phi_c = \pi$ and (d) $\phi_c = 1.5\,\pi$. (c.f. Fig. 4 in [2]).

A. Coherent field

We start the numerical analysis of the system driven by a quantized field by assuming that initially the driving field is in a coherent state

$$C_3^n(0) = e^{-|\alpha|^2/2}\frac{\alpha^n}{\sqrt{n!}}\,, \qquad \alpha = |\alpha|\,e^{i\phi_\alpha}\,. \qquad (19)$$

We thus have two phases in our system: ϕ is the phase of the coupling constant $\bar{g}$, and ϕ_α is the phase of the initial coherent state. Note that $|\alpha|^2$ is the average number of photons in the driving field mode, which for strong coherent fields can be used to relate the classical Rabi frequency to the quantum counterpart via the equation $|\Omega| = |\bar{g}|\cdot|\alpha|$, as $|\alpha| \approx |\alpha| \pm 1$ for $|\alpha| \gg 1$ in the semiclassical limit. Then, using the same values for $|\Omega|$ and ω_{21} as in the reference Fig. 3, we vary the phases ϕ and ϕ_α. The results are shown in Table I. In summary, the quantum simulation with a coherent state as initial state of the driving field mode yields identical results to the classical calculation if one identifies the phases as follows:

$$\phi + \phi_\alpha \leftrightarrow \phi_c\,. \qquad (20)$$

One may intuitively understand this result by taking the expectation value of the quantum interaction Hamiltonian $V_{\rm drive}$ for the coherent state $|\alpha\rangle$:

$$\langle\alpha|\,V_{\rm drive}\,|\alpha\rangle = i\hbar\,(\bar{g}\,\alpha\,A_{21} - \bar{g}^*\,\alpha^*\,A_{12}) \qquad (21)$$

A comparison with the classical Hamiltonian Eq. (18) again yields $|\Omega| = |\bar{g}|\cdot|\alpha|$ and the phase relation Eq. (20). Thus, in a quantized description of a classical driving field with a fixed phase, the classical phase may either be attributed to the coupling constants or to the initial field state.

	$\phi = 0$	$\phi = \pi/2$	$\phi = \pi$
$\phi_\alpha = 0$	a)	b)	c)
$\phi_\alpha = \pi/2$	b)	c)	d)
$\phi_\alpha = \pi$	c)	d)	a)

TABLE I: Results of the numerical simulation of the system in Fig. 1 driven by a quantized field which initially is in a coherent state with phase ϕ_α. ϕ is the phase of the coupling constant $\bar{g}$. In the table, e.g. a) means that the result for this phase configuration is identical to reference a) in Fig. 3.

B. Single Fock mode

We now study the system where the quantized driving field initially is in a single Fock mode:

$$C_3^n(0) = \delta_{n,n_0}\,. \qquad (22)$$

Here δ_{ij} is the Kronecker delta symbol, and n_0 is the photon number of the Fock state initially populated. The resulting spontaneous emission spectrum is shown in Fig. 4. It does not depend on the phase ϕ, which is reasonable, as a number state does not possess a definite phase [24]. The obtained spectrum is essentially a sum of four independent Lorentzian structures which correspond to the four transitions from the upper state to the corresponding dressed states as shown in Fig. 2. It turns out that the spectrum for a single Fock state is identical to the spectrum obtained for a coherent or classical driving field if the interference effects are ignored. This can either be done by removing the corresponding terms from the equations of motion, or by averaging the emission spectrum over all possible values of the phase ϕ. Thus no interference occurs for a single Fock mode.

C. Adjacent Fock modes

Next we consider a driving field where few adjacent Fock states are initially populated with a fixed phase relation, for simplicity with equal weight:

$$C_3^n(0) = \frac{1}{\sqrt{2W+1}}\sum_{k=-W}^{W} e^{i\,k\,\phi_\alpha t}\,\delta_{n,n_0+k}\,. \qquad (23)$$

Here, W is the width of the initial Fock mode distribution around photon number n_0. For this initial configuration, the resulting emission spectra are qualitatively similar to the ones shown in Fig. 3, even for $W = 1$. In particular, the phase dependence is the same. Quantitatively, there are deviations from the classical spectrum for low W, which disappear with increasing W. The reason for these deviations is given in Sec. IV.

D. Separated Fock modes

Finally we study the case where N non-adjacent Fock states are initially populated, again with equal weight for simplicity:

$$C_3^n(0) = \frac{1}{\sqrt{N}} \sum_{k=1}^{N} e^{i\,\kappa_k\,\phi_\alpha t}\,\delta_{n,n_0+\kappa_k}\,. \qquad (24)$$

Here, κ_k is a set of N photon numbers with $|\kappa_i - \kappa_j| > 1$ for all $1 \le i \ne j \le N$. Thus if for arbitrary n one has $C_3^n(0) \ne 0$, then $C_3^{n+1}(0) = 0$ and $C_3^{n-1}(0) = 0$. In this case, the result is equal to the result for a single Fock mode, i.e. there is no interference independence of the width $[\max_k(\kappa_k) - \min_k(\kappa_k)]$ of the initial photon number distribution.

IV. DISCUSSION

In order to understand the results of the above Section III, it is important to note that even though the driving field is assumed to couple the two lower states only, the upper state atomic state $|3\rangle$ also splits up in a multiplet of states $|3, n\rangle$ which decays into the corresponding dressed states. Fig. 5 shows all the possible decay pathways from three adjacent upper states $|3, n+1\rangle$, $|3, n\rangle$ and $|3, n-1\rangle$. First, we assume that only state $|3, n\rangle$ is populated, i.e. a single Fock mode. Then Fig. 5 shows that

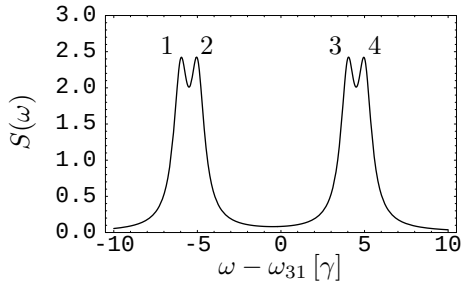

FIG. 4: Spontaneous emission spectrum without interference. This figure is either obtained for a single Fock mode as initial state of the driving field, or by averaging the spectrum for a coherent driving field over all possible values of the phase. The parameters are as in Fig. 3. The numbers at the peaks correspond to the transitions indicated in the dressed state picture of the system in Fig. 2.

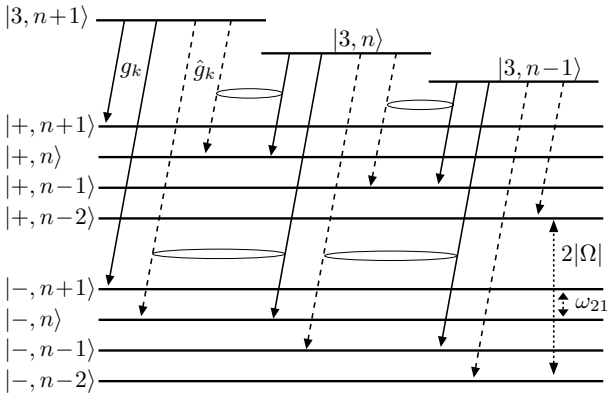

FIG. 5: Decay pathways starting from single upper state Fock modes $|3, n\rangle$ into the corresponding lower dressed states. The solid (dashed) arrows are decays due to coupling via coupling constant g_k ($\hat{g}_k$). The ellipses mark interfering pathways. The parameters are chosen as in Fig. 3, such that the AC-Stark splitting $|\Omega|$ is larger than the photon frequency splitting ω_{21}, as indicated by the double arrows.

each of the possible final states is only reached via a single pathway from the initial state. Thus no interference is possible, in accordance with the results in Section III. Next we assume that all three adjacent upper states $|3, n\rangle$ and $|3, n\pm1\rangle$ are populated. Then some of the final states can be reached via two pathways, as indicated by the ellipses in Fig. 5, which gives rise to interference effects. It is interesting to note that the two initial states of the interfering pathways are different, only the final state is the same. The two initial states, however, have a fixed phase relation with relative phase ϕ, which nevertheless allows for interference to take place. The interfering subsystems are thus independent three-level systems in V configuration. Note that independent interference to several final states was also found in other systems [23]. This conclusion can be further verified by noting from Fig. 5 that for each final state, one of the pathways is mediated by the coupling constant g_k, whereas the other path is proportional to $\hat{g}_k$. Thus the interference effects should also be controllable via the relative phase of these coupling constants just as via the phase ϕ. A numerical check shows that this is indeed the case.

The interference mechanism in the subsystems in V configuration, however, is not completely analogous to the well-known spontaneous-emission interference in V systems with parallel transition dipole moments (see e.g. [25]). This is illustrated in Fig. 6. There, the interference structure around $\omega - \omega_{31} = 5$ in Fig. 3(a) is shown again, but for different values of ω_{21}. It can be seen that perfect interference, i.e. a vanishing of the spectral intensity at a certain frequency, only occurs for curve (iii) with $\omega_{21} = \gamma$. The interference effects are reduced both if ω_{21} is increased or decreased. This is in contrast to the usual V system with parallel dipole moment, where the interference effects only become smaller if the level spacing is increased. This upper restriction to ω_{21} warrants that

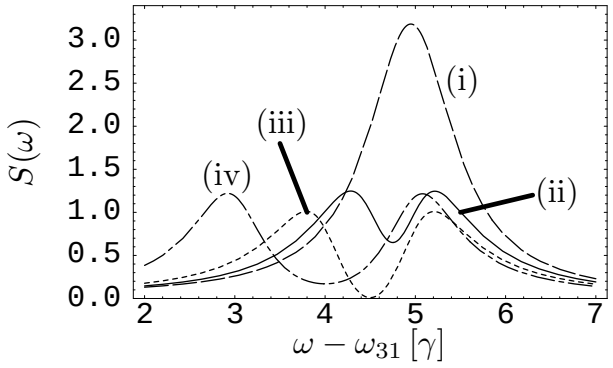

FIG. 6: Dependence of the interference effects on the lower state separation ω_{21}. The parameters are as in Fig. 3(a), except for (i) $\omega_{21} = 0.1$, (ii) $\omega_{21} = 0.5$, (iii) $\omega_{21} = 1$, (iv) $\omega_{21} = 2$.

the interfering pathways cannot be distinguished by their transition frequencies. In our system, the additional requirement $\omega_{21} \approx \gamma$ for maximum interference stems from the fact that for total destructive interference, the two amplitudes must have equal weights. This is the case for $\omega_{21} = \gamma$. Thus the analogy to spontaneous decay in atomic V systems with non-orthogonal transition dipole moments in [25] is not complete.

In Section III, we found that for small numbers of adjacent Fock states initially populated, there is a quantitative deviation of the spectrum from the classical case. The reason for this is that the decay pathways which do not take part in an interfering V subsystem disturb the spectrum. For a narrow distribution with equal weights, the relative weight of the disturbing pathways is not negligible as compared to the weight of the interfering pathways such that the quantum spectrum deviates from the classical one. If the number of adjacent states initially populated grows, the relative weights of the disturbing paths become small, and the spectrum approaches the classical one. A nice check is possible by considering three adjacent states $n, n \pm 1$ populated initially as in Fig. 5, but evaluating the spectrum with amplitudes α_n and β_n only. The result is a spectrum identical to the classical one up to a normalization factor $1/|C_3^n(0)|^2$, as then only the interfering pathways are taken into account, while the contribution of the disturbing final states which are only populated by a single pathway are neglected.

From Fig. 5 and from the definition of the dressed states in Eq. (5) one may also understand why it is not possible to cancel the spontaneous emission completely. On evaluating the transition matrix elements between upper states $|3, n\rangle$ and the dressed states $|\pm, n\rangle$ for spontaneous emissions, one finds that the relative phase between paths leading to dressed states $|+, n\rangle$ differs by π from the relative phase between paths leading to dressed states $|-, n\rangle$. Thus destructive interference is not possible to both dressed state manifolds at the same time, and there is always spontaneous emission.

Finally, we discuss the case of distant Fock modes initially populated. As can be seen from Fig. 5, then none of the final states can be reached via more than one pathway, and no interference is possible. Thus it is not a large total width of the initial driving field state, but rather the fixed phase relation between adjacent Fock mode states, which accounts for the interference effects.

In summary, we have discussed the spontaneous-emission spectrum of a three-level system in Λ configuration, which is sensitive to the phase of a quantized electromagnetic field coupling the two lower atomic states. The quantum treatment together with a specific choice of non-classical initial states for the driving field allows to identify the mechanism leading to interference and the phase dependence. We found that the quantized driving field creates an upper-state multiplet of Fock number states. The system shows interference signatures if the initial state of the driving field contains adjacent Fock number states with a fixed phase relation. The reason for this condition is that then the full level spectrum contains three-level subsystems in V configuration which allow for pathways interference on the two transitions to the lower state. Each of these V systems is made up from two states of the upper state multiplet and a lower dressed state.

APPENDIX A: DERIVATION OF EQ. (11)

In this appendix, we briefly outline the derivation of the solution to the upper state amplitude equation of motion given in Eq. (11). For this, we introduce the variables

$$X_k^n = \frac{1}{\sqrt{2}} \left(\alpha_k^n + \beta_k^n\right) , \tag{A1}$$

$$Y_k^n = \frac{1}{\sqrt{2}} \left(\alpha_k^n - \beta_k^n\right) . \tag{A2}$$

Then, Eqs. (8)-(10) can be written as

$$\frac{d}{dt} C_3^n = \sum_k g_k \, e^{-i\delta_k t} \, X_k^n + i \sum_k \hat{g}_k \, e^{i\phi} \, e^{-i\hat{\delta}_k t} \, Y_k^n , \tag{A3}$$

$$\frac{d}{dt} X_k^n = - g_k^* \, e^{i\delta_k t} \, C_3^n - i \, |\bar{g}| \, \sqrt{n} \, Y_k^{n-1} , \tag{A4}$$

$$\frac{d}{dt} Y_k^n = i \, \hat{g}_k^* \, e^{-i\phi} \, e^{i\hat{\delta}_k t} \, C_3^n - i \, |\bar{g}| \, \sqrt{n+1} \, X_k^{n+1} . \tag{A5}$$

The equations for X_k^n and Y_k^n can be decoupled e.g. by applying a derivation with respect to time to Eq. (A4) and inserting Eq. (A5), which yields:

$$\frac{d^2}{dt^2} X_k^n = - |g|^2 \, n \, X_k^n - g_k^* \frac{d}{dt} \left(e^{i\delta_k t} \, C_3^n\right) + \hat{g}_k^* \, \bar{g}^* \, \sqrt{n} \, e^{i\hat{\delta}_k t} \, C_3^{n-1} . \tag{A6}$$

The further treatment of this equation is simplified by noting that $X_k^n(0) = 0 = Y_k^n(0)$, as we assume the atom

to be in the excited state $|3\rangle$ initially. We can then write the solution of Eq. (A6) as

$$X_k^n(t) = -g_k^* \int_0^t e^{i\delta_k \tau} \cos[v_n(t-\tau)]\, C_3^n(\tau)\, d\tau + \hat{g}_k^*\, e^{-i\phi} \int_0^t e^{i\hat{\delta}_k \tau} \sin[v_n(t-\tau)]\, C_3^{n-1}(\tau)\, d\tau\,, \tag{A7}$$

with $v_n = |g|\sqrt{n}$. An analogous calculation yields

$$Y_k^n(t) = i\hat{g}_k^*\, e^{-i\phi} \int_0^t e^{i\hat{\delta}_k t} \cos[v_{n+1}(t-\tau)]\, C_3^n(\tau)\, d\tau + i g_k^*\, e^{-i\phi} \int_0^t e^{i\delta_k t} \sin[v_{n+1}(t-\tau)]\, C_3^{n+1}(\tau)\, d\tau\,. \tag{A8}$$

Inserting Eqs. (A7), (A8) in Eq. (A3), one obtains

$$\begin{aligned}\frac{d}{dt} C_3^n(t) = & -\sum_k |g_k|^2 \int_0^t e^{-i\delta_k(t-\tau)} \cos[v_n(t-\tau)]\, C_3^n(\tau)\, d\tau \\ & -\sum_k |\hat{g}_k|^2 \int_0^t e^{-i\hat{\delta}_k(t-\tau)} \cos[v_{n+1}(t-\tau)]\, C_3^n(\tau)\, d\tau \\ & +\sum_k g_k\, \hat{g}_k^*\, e^{-i\phi} \int_0^t e^{-i\delta_k(t-\tau)}\, e^{i\omega_{21}\tau} \times \sin[v_n(t-\tau)]\, C_3^{n-1}(\tau)\, d\tau \\ & -\sum_k g_k^*\, \hat{g}_k\, e^{i\phi} \int_0^t e^{-i\delta_k(t-\tau)}\, e^{-i\omega_{21}\tau} \times \sin[v_{n+1}(t-\tau)]\, C_3^{n+1}(\tau)\, d\tau\,. \end{aligned} \tag{A9}$$

Here, the last two terms are interference cross terms which are present as the two transition dipole moments are assumed to be non-orthogonal. Equation (A9) can be evaluated in a Wigner-Weisskopf-like analysis to

$$\frac{d}{dt} C_3^n(t) = -\frac{\gamma}{2} C_3^n(t)\,, \tag{A10}$$

where $\gamma = 2\pi[D(\omega_{31})\, g(\omega_{31})^2 + D(\omega_{32})\, \hat{g}(\omega_{32})^2]$ is the total upper state decay rate. Note that the Wigner-Weisskopf procedure gives rise to a delta function $\delta(t-\tau)$ in the integrand, such that the interference cross terms containing a sine function in Eq. (A9) vanish. Thus the upper state decay is not affected by the fact that the two transition dipole moments are assumed to be parallel.

[1] Z. Ficek and S. Swain, *Quantum Interference and Coherence: Theory and Experiments* (Springer, Berlin, 2005).
[2] M. A. G. Martinez, P. R. Herczfeld, C. Samuels, L. M. Narducci, and C. H. Keitel, Phys. Rev. A **55**, 4483 (1997).
[3] T. Quang, M. Woldeyohannes, S. John, and G. S. Agarwal, Phys. Rev. Lett. **79**, 5238 (1997);.
[4] E. Paspalakis and P. L. Knight, Phys. Rev. Lett. **81**, 293 (1998).
[5] S.-Q. Gong, E. Paspalakis, and P. L. Knight, J. Mod. Opt. **45**, 2433 (1998).
[6] Z. Ficek, J. Seke, A. Soldatov, and G. Adam, Optics Commun. **182**, 143 (2000).
[7] D. Bortman-Arbiv, A. D. Wilson-Gordon, and H. Friedmann, Phys. Rev. A **63**, 043818 (2001).
[8] J.-H. Wu and J.-Y. Gao, Phys. Rev. A **65**, 063807 (2002).
[9] G. Morigi, S. Franke-Arnold, and G.-L. Oppo, Phys. Rev. A **66**, 053409 (2002).
[10] M. Macovei, J. Evers, and C. H. Keitel, Phys. Rev. Lett. **91**, 233601 (2003); Phys. Rev. A **71**, 033802 (2005).
[11] M. Sahrai, H. Tajalli, K. T. Kapale, and M. S. Zubairy, Phys. Rev. A **70**, 023813 (2004).
[12] M. A. Macovei and J. Evers, Opt. Comm. **240**, 379 (2004).
[13] W. H. Xu, J. H. Wu, and J. Y. Gao, Laser Phys. Lett. **1**, 176 (2004).
[14] V. S. Malinovsky and I. R. Sola, Phys. Rev. Lett. **93**, 190502 (2004).
[15] F. Ghafoor, S.-Y. Zhu, and M. S. Zubairy, Phys. Rev. A **62**, 013811 (2000).
[16] S.-Y. Gao, F.-L. Li, and S.-Y. Zhu, Phys. Rev. A **66**, 043806 (2002).
[17] S. Menon and G. S. Agarwal, Phys. Rev. A **57**, 4014 (1998).
[18] E. A. Korsunsky, N. Leinfellner, A. Huss, S. Baluschev, and L. Windholz, Phys. Rev. A **59**, 2302 (1999).
[19] J. Evers and C. H. Keitel, Phys. Rev. Lett. **89**, 163601 (2002); P. R. Berman, Phys. Rev. Lett. **92**, 159301 (2004); A. G. Kofman, Phys. Rev. Lett. **92**, 159302 (2004). J. Evers and C. H. Keitel, Phys. Rev. Lett. **92**, 159303 (2004).
[20] J. Evers and C. H. Keitel, J. Phys. B: At. Mol. Opt. Phys. **37**, 2771 (2004).
[21] U. Akram, J. Evers, and C. H. Keitel, J. Phys. B **38**, L69 (2005).
[22] M. O. Scully and M. S. Zubairy, *Quantum Optics* (Cambridge University Press, Cambridge, 1997).
[23] J. Evers, D. Bullock, and C. H. Keitel, Opt. Comm. **209**, 173 (2002).
[24] R. Loudon, *The Quantum Theory of Light* (Oxford University Press, Oxford, 2000).
[25] S. Y. Zhu, R. C. F. Chan, and C. P. Lee, Phys. Rev. A **52**, 710 (1995).